Genes & Diseases (2019) 6, 407–418

Available online at www.sciencedirect.com

ScienceDirect

journal homepage: http://ees.elsevier.com/gendis/default.asp

FULL LENGTH ARTICLE

Identification and characterization of the cellular subclones that contribute to the pathogenesis of mantle cell lymphoma

Junling Tang [a,b], Li Zhang [c], Tiejun Zhou [d], Zhiwei Sun [a], Liangsheng Kong [a], Li Jing [b], Hongyun Xing [b], Hongyan Wu [b], Yongli Liu [a], Shixia Zhou [a], Jingyuan Li [a], Mei Chen [b], Fang Xu [e], Jirui Tang [b], Tao Ma [b], Min Hu [b], Dan Liu [b], Jing Guo [b], Xiaofeng Zhu [b], Yan Chen [b], Ting Ye [a], Jianyu Wang [a,***,1], Xiaoming Li [b,**,1], H. Rosie Xing [a,f,*,1]

[a] *Laboratory of Translational Cancer Stem Cell Research, Institute of Life Sciences, Chongqing Medical University, 1 Yixueyuan Rd, Chongqing, 400016, China*
[b] *Department of Hematology, The Affiliated Hospital of Southwest Medical University, 25 Tai Ping Street, Luzhou, 646000, China*
[c] *The Affiliated Stomatology Hospital of Southwest Medical University, 2 Jiangyangnan Rd, Luzhou, 646000, China*
[d] *Department of Pathology, The Affiliated Hospital of Southwest Medical University, 25 Tai Ping Street, Luzhou, 646000, China*
[e] *Department of Hematology, Mianyang Central Hospital, 12 Changjia Lane, Jingzhong Street, Mianyang, 621000, China*
[f] *School of Biomedical Engineering, Chongqing Medical University, 1 Yixueyuan Rd, Chongqing, 400016, China*

Received 5 November 2018; accepted 17 December 2018
Available online 21 December 2018

KEYWORDS
JeKo-1-spheroid;
Mantle cell

Abstract Mantle cell lymphoma (MCL) is a B-cell malignancy with poor clinical outcome and undefined pathogenesis. Development of clinically relevant cellular models for MCL research is an urgent need. Our preliminary observations lead the development of two novel hypotheses that we tested in this study: 1. multicellular spheroid might be a unique growth mode of early-

* Corresponding author. Laboratory of Translational Cancer Stem Cell Research, Institute of Life Sciences, Chongqing Medical University, 1 Yixueyuan Rd, Chongqing, 400016, China.
** Corresponding author.
*** Corresponding author.
E-mail addresses: Wjy2003123@163.com (J. Wang), zlroy2003@163.com (X. Li), Xinglab310@163.com.CELL (H.R. Xing).
Peer review under responsibility of Chongqing Medical University.
[1] These authors contributed equally.

https://doi.org/10.1016/j.gendis.2018.12.002

lymphoma;
Pathology;
Sub-clone;
CD19

stage cells in MCL; 2. MCL might be a polyclonal tumor. We made the following original observations that have not been reported: First, we have provided a new experiment method for enriching MCL early-stage cells and characterized the spheroid mode of growth as a unique feature of early-stage MCL cells in cell line as well as in clinical samples. Second, we have established a clinically relevant cellular model of MCL, the *JeKo-1-spheroid* cell line, that was highly enriched in early-stage sub-clones. *JeKo-1-spheroid* cells and the spheroid growing cells enriched from MCL patients exhibited comparably enhanced tumorigenic abilities and similar biological features. Third, Immunophenotypic analysis has revealed that MCL may be derived from precursor-B(pre-B), immature-B and mature-B cells, not only the mature-B cells as WHO classified in 2016. Fourth, MCL may be a polyclonal disease composed of $CD19^{-}/IgM^{-}$, $CD19^{-}/IgM^{+}$, $CD19^{+}/IgM^{+}$ three sub-clones, of which the $CD19^{-}/IgM^{+}$ sub-clone might be the dominant sub-clone with the strongest tumorigenic ability. Fifth, $CD19^{+}/IgM^{-}$ that differentiates MCL and normal B cells may represent a new marker for MCL early detection, minor residual disease monitoring after therapies and prognosis.

Introduction

The study of clonal evolution is one of the frontiers in hematologic cancer research. Majority of the work in this area has been conducted in leukemia research.[1–3] A case of co-occurrence of Hodgkin lymphoma (HL) and MCL in the same patient suggests sub-clonal evolution of HL from MCL.[4] Moreover, the heterogeneity within MCL tumors and resistance to therapies imply that the MCL tumors are comprised of the cells with different tumorigenic capacities.[5] These observations suggest that MCL might be polyclonally-driven.[6] However, existing experimental evidence fails to explain the complexities of clonal dynamics in hematologic cancer.[7]

While the majority of prior studies hypothesized the mature B cells as the origin of MCL based on the expression of CD19 and IgM,[8–10] few studies have postulated otherwise that CD19-negative ($CD19^{-}$) B cells are the initiating cells.[5,11] Early studies employed differentiation markers to identify the mature and immature cell for common hematological diseases: CD138 for multiple myeloma (MM),[12] CD19 for MCL[5,11] and CD34 for acute leukemia (AL).[13] More recent studies used whole-genome sequencing,[2] array comparative genomic hybridization,[6] and light chain research[14] to study malignant progression of hematologic cancer. Studies on the pathogenesis of MCL were primarily relied on the cell lines and clinical specimen,[5,7,10] with supplementary animal studies.[11] The *JeKo-1-parental* cell line is the most widely used model of MCL. While it was established from peripheral blood mononuclear cells (PBMCs) of a patient, the genetic make-ups of this cell line and others differ significantly from that of the clinical specimens,[5,15–17] thus findings made in this cell line were largely ignored.

By establishing a cellular model enriched in early stage cells that closely mimic the clinical progression of MCL, we have generated experimental evidence supporting the polyclonal nature of MCL, a finding that has significant clinical implications.

Materials and methods

Cell line and patient sample

The *JeKo-1-parental* and *JeKo-1-spheroid* cell lines were cultured and maintained in RPMI 1640 (HyClone) supplemented with 20% heat-inactivated foetal calf serum (Excell), 2 mM L-glutamine, 50 U/ml penicillin and 50 μg/ml streptomycin. Blood or bone marrow specimens from patients and healthy donors were obtained after informed consent, as approved by Southwest Medical University of Institutional Review Boards. Mononuclear cells were isolated from patients and normal specimens by standard Ficoll gradient methods, and were maintained in methylcellulose (Methocult H4435, Stem Cell Technologies). After three to five generations, the cells were transferred into the same medium as *JeKo-1-parental* cell lines.

Side population assay

The Hoechst 33342 staining procedure was based on the method described by Goodell et al[18] Hoechst 33342 staining was observed using a FACS a flow cytometer (Becton—Dickinson, USA).

Flow Cytometry and sorting

Single-cell suspension cells were incubated with the respective conjugated antibody for 15 min at 4 °C and analyzed with a BD LSR. IgM-APC (catalog: 551062) was from BD Biosciences. CD19-FITC (catalog: 11-0199), CD45-Alexa Fluor 700 (catalog: 56-9459), CD3-PerCP-Cy5.5 (catalog: 45-0037) and CD34-PE-Cyanine 7 (catalog: 25-0349) were from eBioscience. CD38- PerCP-Cy5.5 (catalog: B49199), TDT-PITC (catalog: IM3524), CD22-PE (catalog: IM1835U), CD5-PerCP-Cyanine 5.5 (catalog: B49191), CD19-ECD (catalog: 652804), CD10-PE (catalog: A07760) and CD34-ECD (catalog: IM2709U) were from Beckman Coulter.

Propidium iodide were from Sigma. The gating strategy for MCL cells were selected using $CD19^-/IgM^-$, $CD19^-/IgM^+$ and $CD19^+/IgM^+$cells (gate i: $CD45^+/PI^-$; gate ii: $CD34^-/CD3^-$; gate iii: $CD19^-/IgM^-$, $CD19^-/IgM^+$ and $CD19^+/IgM^+$). The sorting purity was greater than 99% in the majority of samples. All the fractions were isolated by fluorescence-activated cell sorting (Aria, Becton Dickinson, San Jose, CA).

Detection of stem cell- and B cell-associated markers by qRT-PCR

Total RNA was extracted with TRIZOL (Invitrogen) according to the manufacturer's protocol. A standard RT-PCR was conducted using a PrimeScript RT Master Mix (Takara) according to the manufacturer's instructions.

Colony formation assay (CFA)

Each sorted population was plated in 35-mm^2 dishes with methylcellulose in accordance with the manufacturer's instructions. Cells were incubated for two weeks at 37 °C in a 5% CO2 incubator. The clonogenic spheroids that consisting of a minimum of 40 cells were counted under microscopy.

Xenotransplantation in NOD/SCID mice

All mice used in the study were obtained from the core facility of Experimental Animal Centre, as approved by Animal Care Committee. The *JeKo-1-parental* and *JeKo-1-spheroid* cells were injected intraperitoneally at doses of 10^6 cells per NOD/SCID mouse (n = 4, 27 days). Highly purified $CD19^-/IgM-$, $CD19^-/IgM+$ and $CD19^+/IgM^+$ cells from JeKo-1-spheroid (n = 3, 19 days) and pt4 (n = 4, 9 days) were injected intraperitoneally at two doses 10^2 and 10^4, respectively. Tumor-bearing mice were sacrificed when mice were moribund. The brain, thymus, sternum, heart, lung, liver, spleen, kidney and adrenal gland, stomach, intestines and pancreas were collected for hematoxylin and eosin (H&E) staining, and the spleens were used for immunohistochemistry.

Immunohistochemistry (IHC)

Tissue samples were fixed in 10% buffered formalin phosphate, stored in 70% ethanol, then followed by paraffin embedding. Samples were serially sectioned and stained with H&E, anti-human *IgM* (catalog: ab17104, Abcam), *CD20* (catalog: Kit-0001, Maxim), *CD79a* (catalog: RMA-0552, Maxim), *Ki-67*(catalog: ZA-0502, ZSGB), *CCND1* (catalog: RMA-0541, Maxim) and *Pax5* (catalog: AM0281, Ascend).

Statistical analysis

When two groups were compared, the Student's *t*-test with Welch's correction was used. By default, two-tailed tests were performed. *P < .05 was defined as statistically significant. **P < .0001 were considered highly statistically significant. All statistical analyses were performed using GraphPad Prism version 5.0.

Results

Multicellular spheroid is a unique growth mode of early-stage cells in MCL and the establishment of the JeKo-1-spheroid *cell line*

We found that in the early passages (<10 passages), the *JeKo-1-parental* cells was made of primarily single cells. However, there were approximately 1% of cells grew as multicellular spheroids (Fig. 1A). FCM analysis revealed that the ratio of $CD19^-$ B cells was 0.34% ± 0.07% (Fig. 1B, C) in *JeKo-1-parental* cells. As the culture prolonged (10—20 passages), the majority of single cells gradually died (Fig. 1A, C) and the surviving cells formed irregular-shaped multicellular spheroids (Fig. 1A). However, around the twentieth generation, towards the end of the batch cell death, the irregular spheroids became regularly-sized. We evaluated the cell viability by the ratio of propidium iodide negative (PI^-) using FCM for the different growth modes. Cell viability decreased from 94.32% ± 0.86% in single-cell suspension growth phase to 63.77% ± 1.90% in the irregular multicellular spheroid mode of growth, but was restored to 96.12% ± 0.78% in the stable spheroid mode of growth (>20th passage, Fig. 1C, D). When sorted $CD19^-$ and $CD19^+$cells were cultured in *vitro*, $CD19^+$ cells grew as single-cell suspension and died within 2—3 weeks, while the $CD19^-$ cells retained high cell viability and grew slowly as small spheroid for 3—4 weeks (data not shown). We named this derivative cell line the *"JeKo-1-spheroid"*. The *JeKo-1-spheroid* consisted mostly the spheroids with only a few single cells (Fig. 1A) and could be serially passaged more than 100 generations with efficient recovery after freezing in liquid nitrogen. To assess the clinical relevance, we harvested and isolated fresh MCL cells from two patients (pt1, pt2) and cultured them under the same condition of *JeKo-1-parental cells*. The primary cultures of MCL clinical samples were also dominated by spheroid growth (Fig. 1E). Maintenance of hematological cancer cell in single-cell suspension culture for biological studies is the standard practice. However, spheroid growth has been a characteristic feature of stem-like cells isolated from solid tumor in serum-free culture condition.[19,20] These findings prompt us to hypothesize that: "spheroid growth is a unique feature of early-stage cells in MCL". To test this hypothesis and to identify the cellular make-up of the spheroids, we used FCM to measure $CD19^-$ content. The proportion of $CD19^-$ cells was 0.34% ± 0.07% in *JeKo-1-parental* cells, it increased to 88.97% ± 3.50% in *JeKo-1-spheroid*, a total of 261 times enrichment (Fig. 1B, C). Comparable level of enrichment of $CD19^-$ population in clinical samples was achieved (98.46% ± 0.74%, Fig. 1B).

We also conducted analysis of side population (SP) cells by FCM—based Hoechst 33342 staining.[18] SP cells are enriched source of cancer-initiating cells with stem cell properties, which have been identified in solid tumors and hematopoietic malignancies.[21] Similar to the enrichment of $CD19^-$ cell population in *JeKo-1-spheroid*, SP population was increased 108 times, from 0.11% ± 0.01% in *JeKo-1-*

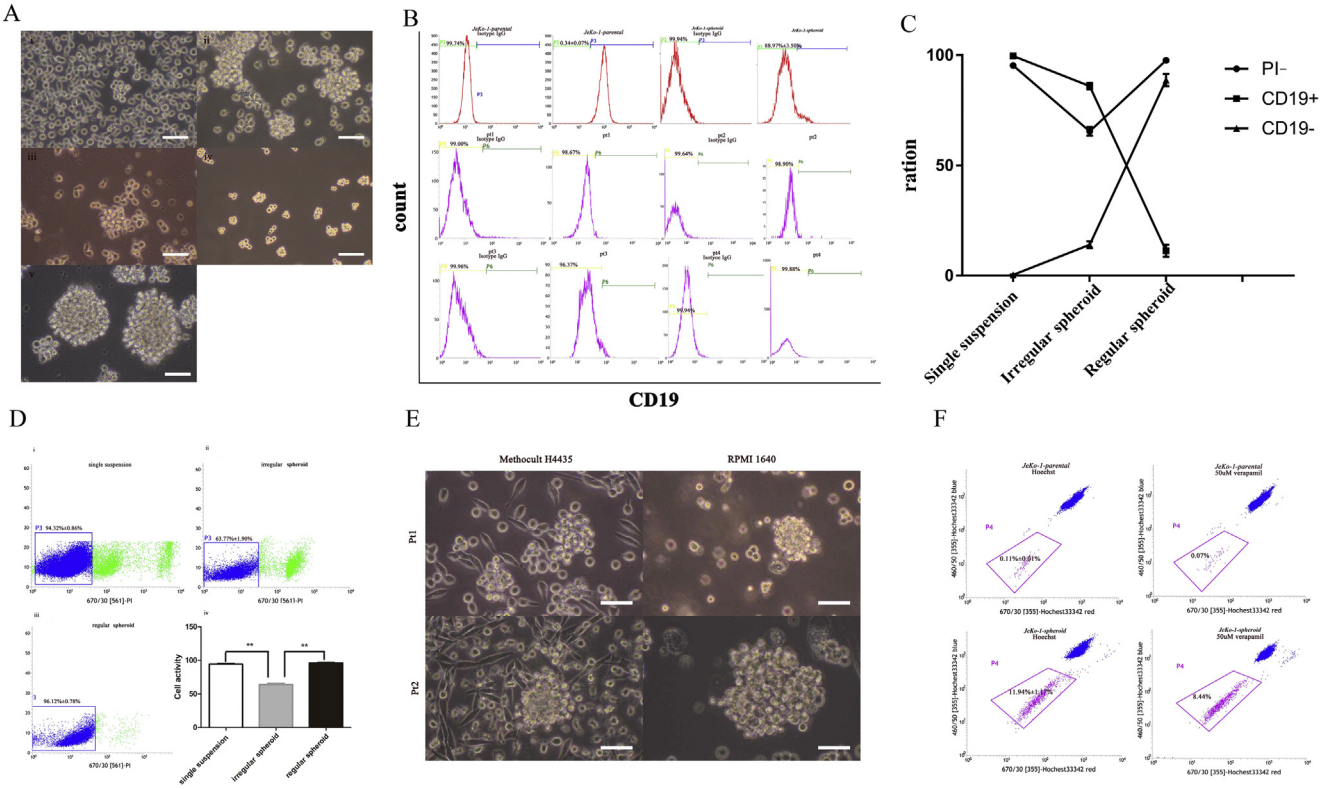

Figure 1 Evolution of Biological characteristics between *JeKo-1-parental* and *JeKo-1-spheroid* cells. (A)The growth characteristics of *JeKo-1-parental* and *JeKo-1-spheroid* cell lines; there were approximately 1% multicellular spheroid in *JeKo-1-parental* culture (i); irregular multicellular spheroid in *JeKo-1-parental* prolonged culture (ii); death of single cells in *JeKo-1-parental* prolonged culture (iii); restoration of proliferation (iv); establishment of *JeKo-1-spheroid* culture (v); bar = 60um.**(B)** The expression of $CD19^{-}$ in *JeKo-1-spheroid* cells, *JeKo-1-parental* cells, patient samples (pt1, pt2, pt3 and pt4). Data are expressed as mean percentage of $CD19^{-}$ cells ± s.d. **(C)** The dynamics of phenotypic proportions of $CD19^{-}$, $CD19^{+}$ and PI^{-} in the three distinct growth modes in *JeKo-1-parental* and *JeKo-1-spheroid* cells. **(D)** The expression of PI^{-} cells in single suspension (i), irregular spheroid (ii) and regular spheroid (iii) growth modes in *JeKo-1-parental* and *JeKo-1-spheroid*; cell viability analysis (iv). Data are expressed as mean percentage of PI^{-} cells ± s.d. **(E)** Multicellular spheroid derived from pt1 and pt2 cultured in Methocult H4435(left); or in RPMI 1640 (right); bar = 60 um. **(F)** Characterization of SP heterogeneity in the panel of *JeKo-1-parental* and *JeKo-1-spheroid* cell lines. Dot plots show control *JeKo-1-parental* and *JeKo-1-spheroid* cells incubated in Hoechst 33342 alone (left), Hoechst 33342 accumulation in the presence of 50 μM verapamil (right). Data are expressed as mean percentage of SP cells ± s.d.

parental cell to 11.94% ± 1.17% in *JeKo-1-spheroid* (Fig. 1F). The proportion of SP cells was decreased by verapamil (50 μM) in *JeKo-1-parental* and *JeKo-1-spheroid* were 0.07%, 8.44% respectively (Fig. 1F), confirming the specificity of the findings.

Collectively, these results demonstrate that multicellular spheroid is a unique growth mode of early-stage cells in MCL (Fig. 1A). The novel cell line, the *JeKo-1-spheroid*, was enriched of $CD19^{-}$ early-stage cells and SP cells (Fig. 1B, F).

Immunophenotypic characterization of the JeKo-1-spheroid *cell line and identification of the three distinct sub-clones*

We conducted immunophenotypic analysis of *JeKo-1-spheroid* by multi-color FCM in order to determine the origin of cells that involved in MCL pathogenesis. The expression of CD34, CD38, TDT, CD22, CD5, CD10 and IgM[22] was evaluated in $CD19^{-}$ cells (Fig. 2A, B), and the expression profile was compared to that of normal B cell differentiation stage (Fig. 2C). The negative expression of CD22 indicated that B cell differentiation antigens were not expressed in $CD19^{-}$ cells. The absence of CD34, CD38 and TDT expression in $CD19^{-}$ cells excluded the cellular origin of normal hematopoietic stem cells, lymphoid common progenitor cells and progenitor B cells, thereby demonstrated that *JeKo-1-spheroid* culture didn't contain these cells.

The expression of CD34, CD10 and CD5 was consistent with the immunophenotype of MCL (Fig. 2A).[23,24] Further, the expression of CD34, CD38, IgM, TDT and CD10 (Fig. 2A, B) in *JeKo-1-spheroid cells* was consistent with the immunophenotype of pre-B, immature B and mature B cells(Fig. 2C), suggesting that MCL pathogenesis might not be limited to mature B cells.[8–10] It may involve cells from multiple differentiation stages (Fig. 2C). We also found that

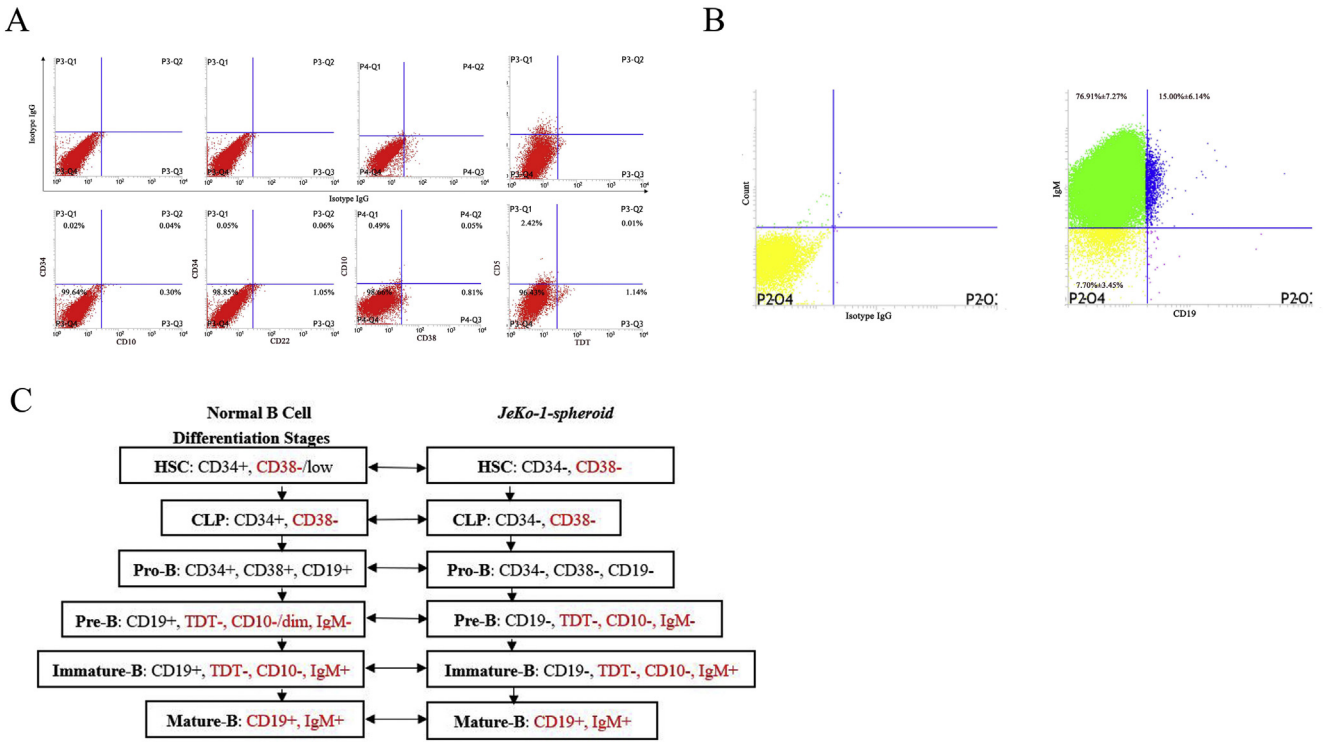

Figure 2 **Immunophenotype analysis of *JeKo-1-parental* and *JeKo-1-spheroid* cells. (A)** The expression of CD22, CD34, CD10, CD5, CD38 and TDT in $CD19^{-}$ population from *JeKo-1-spheroid* cells. **(B)** The expression of CD19 and IgM in *JeKo-1-spheroid* total cells. **(C)** Comparison of marker expression in *JeKo-1-spheroid* with the normal B cell differentiation stages. Red font indicates the same immunophenotype.

CD19 is only expressed in the mature B cells in *JeKo-1-spheroid*, which are not consistent with the normal B cell differentiation. However, CD19 expression is gradually increased from pre-B to immature B and to mature B cell differentiation. Thus, the negative expression of CD19 in the early stage of B-cell may also be a sign of poor differentiation.

Finally, we identified the presence of the three subpopulations with the immunophenotype of $CD19^{-}/IgM^{-}$, $CD19^{-}/IgM^{+}$, and $CD19^{+}/IgM^{+}$, corresponding to pre-B, immature B and mature B cells, respectively (Fig. 2B, C).

JeKo-1-spheroid *cell line exhibited enhanced oncogenic potential*

The transcription of *Oct2*, *bcl-9*, *bcl-2*, *bcl-11b*, *c-myc*,*CCND1*, *bcl-11a*, *bmi-1*, *sox2*, *CD133* and *nanog* was analyzed by qRT-PCR (Table 1). *JeKo-1-spheroid* cells displayed low expression of the mature B cell transcription regulatory factor *Oct2* (Fig. 3A), corroborating the results from immunophenotyping analysis that *JeKo-1-spheroid* cell line was enriched for immature B cells. In contrast, *JeKo-1-spheroid* cells showed elevated expression of the

Table 1 PCR primer sequence.

Gene name	Forward primers	Reverse primers
Bcl-9	AGAGAGAAGCACAGCGCCTC	CTGCAGTCTGGTATTCTGGGAAG
Bcl-2	TTTGAGTTCGGTGGGGTCAT	TGACTTCACT TGTGGCCCAG
Bmi 1	TGTGTGCTTTGTGGAGGGTA	GGTCTGGTCTTGTGAACTTGG
Bcl-11b	TCAAATGAACTTCCCCTTGG	ACCTGCAATGTTCTCCTGCT
Nanog	AGATGCCTCACACGGAGACT	TCTGGAACCAGGTCTTCACC
CD133	GCTTTGCAATCTCCCTGTTG	TTGATCCGGGTTCTTACCTG
C-myc	TTCGGGTAGTGGAAAACCAG	CAGCAGCTCGAATTTCTTCC
Cyclin d1	GATGCCAACCTCCTCAACGAC	CTCCTCGCACTTCTGTTCCTC
Sox 2	CACAACTCGGAGATCAGCAA	GTTCATGTGCGCGTAACTGT
Bcl-11a	ACAAACGGAAACAATGCAATGG	TTTCATCTCGATTGGTGAAGGG
Oct 2	GAAGGAGAAACGCATCAACC	CTTGGGACAACGGTAAGGTC
β-actin	AAGGATTCCTATGTGGGCGACG	GCCTGGATAGCAACGTACATGG

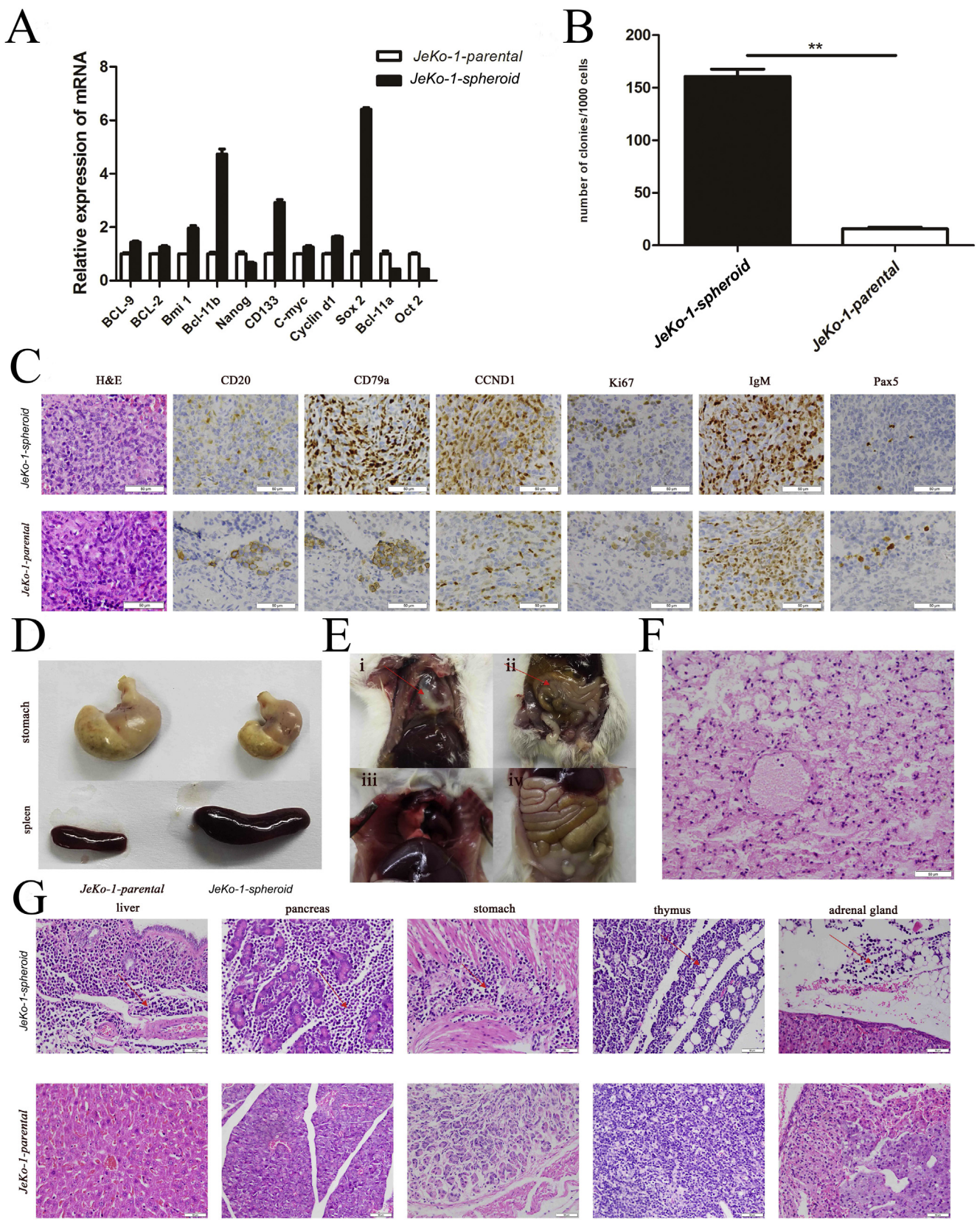

Figure 3 **Tumorigenic potential of *JeKo-1-spheroid* and *JeKo-1-parental* cells. (A)** mRNA expression of stem-cell, oncogene and B-cell differentiation markers in *JeKo-1-spheroid* and *JeKo-1-parental* cells. **(B)** Quantitation of CFA by *JeKo-1-spheroid* and *JeKo-1-parental*. **: $P < .0001$, using the single variance analysis method. **(C)** H&E staining and IHC of *JeKo-1-spheroid* or *JeKo-1-parental*-derived tumour xenografts; bar = 50um. **(D)** Representative images of the stomach and spleen from mice with *JeKo-*

Table 2 Comparative analysis of tumor xenograft induction between *JeKo-1-spheroid* and *JeKo-1-parental*.

Cell	# of mice with tumours	# of tumor-infiltrated organs*	# of infected organs*	# of hemorrhagic organs
Jeko-1-parental	4/4	4/44	2/44	0/44
Jeko-1-spheroid	4/4	11/44	7/44	7/44

oncogenes and stem cell markers including *bcl-9*, *bcl-2*, *bcl-11b*, *sox2*, *CD133*, *c-myc*, *CCND1* and *bmi-1*, consistent with previous report,[25,26] and low expression of *bcl-11a* and *nanog* (Fig. 3A). Overall, our results showed that *JeKo-1-spheroid* cells expressed higher levels of oncogenes and stem cell markers in comparison to the *JeKo-1-parental* cell line.

In order to confirm that *JeKo-1-spheroid* cells has higher clonogenic potential than that of *JeKo-1-parental* cells, we conducted CFA *in vitro* and xenotransplantation assays *in vivo*. The oncogenic potency *in vivo* was assessed by: (1) the number of tumor organs; (2) H&E assessment of bleeding and infection organ, determines the effect of MCL tumor growth on normal hematopoiesis and immune system. In comparison to the *JeKo-1-parental* cells, the *JeKo-1-spheroid* cells formed a significantly higher number of colonies *in vitro* (Fig. 3B).

Xenograft tumors from the two cell lines expressed comparable levels of *CD79a*, *CD20*, *Pax5*, *IgM*, *CCND1* and *Ki-67* proliferation antigens (Fig. 3C).[5] The tumor-invaded stomach of one mice in *JeKo-1-spheroid* group was significantly smaller than the normal stomach in *JeKo-1-parental* group (Fig. 3D). The spleen that had tumor infiltration of one mice in *JeKo-1-spheroid* group was significantly larger than that in *JeKo-1-parental* group (Fig. 3D) with extramedullary hematopoiesis (data not shown), a biological process in order to restore hematopoiesis when bone marrow compensatory function is inadequate. In contrast with normal cardiopulmonary pathology in the *JeKo-1-parental* group, two mice in the *JeKo-1-spheroid* group developed pulmonary infection and bleeding with visible purulent secretion of the red surface (Fig. 3E), with a large number of erythrocytes and neutrophils by H&E staining (Fig. 3F). The pericardial infection in the *JeKo-1-spheroid* group formed an abscess in the heart that caused the cardiopulmonary adhesion (Fig. 3E). Intestinal infections in the *JeKo-1-spheroid* group made the segment of intestine lose its heathy pale pink color, and formed yellow encapsulated abscesses (Fig. 3E). However, none cardiopulmonary infection and hemorrhage occurred in *JeKo-1-parental* group (Fig. 3E). The tabulated data showed that in the *JeKo-1-spheroid* group, the tumor had spread to eleven organs including the spleens, but in the *JeKo-1-parental* group, only spleen was involved without signs of wide disseminated tumor (Fig. 3G; Table 2). There were seven hemorrhagic and infectious organs in *JeKo-1-spheroid* group, in particular, two mice had serious heart and lung infections and hemorrhage, and one mouse had a severe gastrointestinal infection. In comparison, *JeKo-1-parental* group had infections only in two organs and had no organ hemorrhage (Table 2).

In sum, we found that the *JeKo-1-spheroid* cells exhibited enhanced tumor-forming abilities in comparison to the *JeKo-1-parental* cells, that was accompanied by dissemination, severe and extensive complications of infection and hemorrhage which recapitulated the clinical course of MCL progression.

Comparison the oncogenic potential of CD19/IgM sub-populations and the polyclone pathogenesis of MCL

We subsequently compared the oncogenicity of three sub-populations we identified in *JeKo-1-spheroid* cells. The comparative analysis was also performed with sub-populations derived from four patients with stage IV MCL (pt1, pt2, pt3 and pt4) and one healthy donor. We conducted CFA *in vitro* and used three sub-populations of pt4 and *JeKo-1-spheroid* cells in the xenotransplantation assay *in vivo*.

FCM analysis revealed that the healthy donor samples expressed $CD19^-/IgM^-$, $CD19^-/IgM^+$, $CD19^+/IgM^+$ and $CD19^+/IgM^-$ four sub-populations (Fig. 4A; Table 3). In contrast, the $CD19^+/IgM^-$ sub-population was absent in all four clinical specimens and the *JeKo-1-spheroid* cells (Fig. 4A; Table 3). The PBMCs of pt4 were collected from a patient with a large cell variant of MCL showing leukemic conversion which is the terminal stage of MCL. Whereas the other three clinical samples were BMMCs. $CD19^-$ proportion in pt4 sample was as high as 99%, suggesting the importance of $CD19^-$ early-stage clones in MCL disease progression.

CFA analysis demonstrated that all four CD19/IgM sub-populations from one healthy donor were unable to form colonies (data not shown). In contrast, the three sub-populations from pt1, pt2, pt4 and *JeKo-1-spheroid* were all able to form colonies *in vitro* (Figs. 4B, C and 5A—D). In summary, the three sub-populations (henceforth called "sub-clones") in MCL are capable of forming colonies with the relative potency scored in the order as following: $CD19^-/IgM^+ > CD19^+/IgM^+ > CD19^-/IgM^-$(Fig. 4B, C).

We analyzed xenograft tumors by IHC for the expression of *CCND1*, *CD20*, *CD79a*, *PAX 5*, *Ki-67* and *IgM*. The three

1spheroid or *JeKo-1-parental*-derived tumour xenografts. **(E)** Representative images of organs from mice inoculated with *JeKo-1-spheroid* and *JeKo-1-parental*. Red arrows indicate the infected areas from *JeKo-1-spheroid* (upper panel): pulmonary and heart (i), intestine (ii); normal organs from *JeKo-1-parental* (lower panel): pulmonary and heart (iii), intestine (iv). **(F)** H&E staining of pulmonary infection and hemorrhage from mice inoculated with *JeKo-1-spheroid*; bar = 50um. **(G)** Morphological features of the *JeKo-1-spheroid* and *JeKo-1-parental*-derived tumour xenografts; red arrows indicate the tumor lesions from *JeKo-1-spheroid* (upper panel), the normal organs from *JeKo-1- parental* (lower panel); bar = 50um.

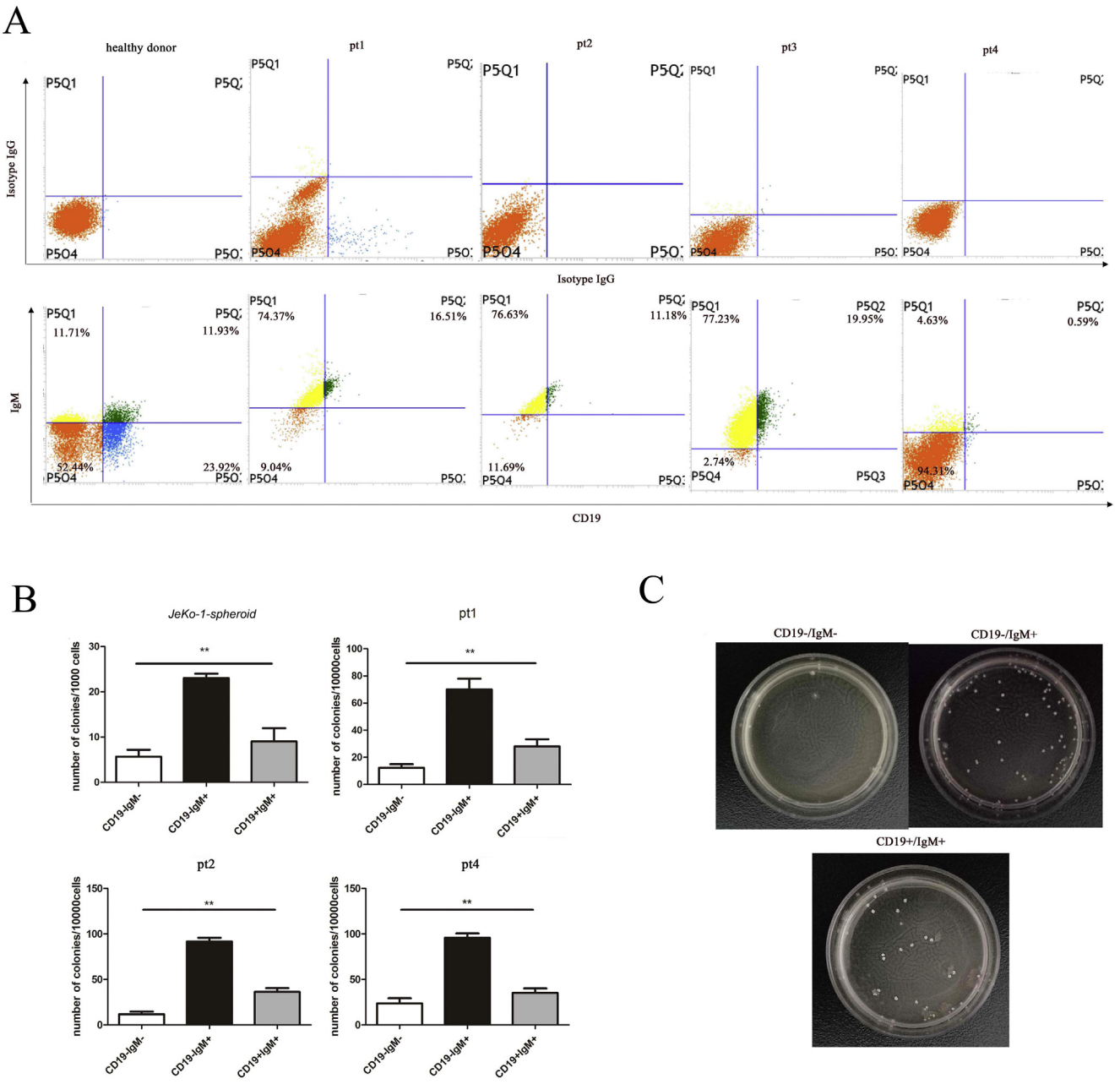

Figure 4 Cancer biology of three sub-clones derived from patients and *JeKo-1-spheroid* cell line. **(A)**The expression of CD19 and IgM in one healthy donor and four MCL patients cells (pt1, pt2, pt3 and pt4). **(B)** Quantitation of colony formation in the three sub-clones from the *JeKo-1-spheroid* cell line, and three clinical samples (pt1, pt2 and pt4). **: $P < .0001$(one-way analysis of variance). **(C)** Representative images of colonies by the three sub-clones from pt 2.

sub-clones isolated from *JeKo-1-spheroid* and pt 4 sample formed tumor masses only in the spleen (Figs. 5A, D and 6A, B), no other organs were involved (Table 4). Nevertheless, the spleen showed the high expression of the genetic hallmark of MCL, *CCND1* (Fig. 6A, B), similar to the high CCND1 expression observed in xenograft tumors derived from the polyclone in *JeKo-1-spheroid* (Fig. 3C). Xenograft tumors from $CD19^{-}/IgM^{-}$, $CD19^{-}/IgM^{+}$ and $CD19^{+}/IgM^{+}$ monoclone from *JeKo-1-spheroid* and pt4 samples didn't showed comparable levels of *CD20*, *CD79a*, *PAX 5*, *Ki-67* and *IgM* (Fig. 6C) markers expressions in comparison to the polyclone in *JeKo-1-spheroid* (Fig. 3C). However, xenograft tumors from monoclones in *JeKo-1-spheroid* and pt 4 sample, and from the polyclone in *JeKo-1-spheroid* all exhibited similar pathological characteristics of MCL, in particular, the presence of small to medium sized lymphoid cells with irregular nuclear contours (Fig. 6A—C).[27]

Together, these data demonstrate that while the monoclones retained *CCND1*-specific high expression, the expression of CD20, CD79a, PAX 5, Ki-67 and IgM couldn't be detected (Fig. 6A—C) and without signs of disseminated tumor. Furthermore, none of the monoclone from *JeKo-1-*

Table 3 Comparison the expression of CD19/IgM sub-populations in *JeKo-1-spheroid*, four patients and healthy donor.

Cells	$CD19^-/IgM^-$(%)	$CD19^-/IgM^+$(%)	$CD19^+/IgM^+$(%)	$CD19^+/IgM^-$(%)
Pt1[a]	9.04	74.37	16.51	0
Pt2[a]	11.69	76.63	11.18	0
Pt3[a]	2.74	77.23	19.95	0
Pt4[b]	94.31	4.63	0.59	0
Jeko-1-spheroid	7.70 ± 3.45	76.91 ± 7.27	15.00 ± 6.14	0
Normal[b]	52.44	11.71	11.93	23.92

[a] BMMCs from patients with clinically confirmed stage IV MCL.
[b] PBMCs from a patient with a large cell variant of MCL showing leukemic conversion and one healthy donor.

spheroid and pt4 was capable of generating xenograft tumors that fully recapitulate the heterogeneity of polyclone tumors in *JeKo-1-spheroid* judged by the total number of organs involved, immune phenotypes and the oncogenic capability (Figs. 3C,D,G and 6A–C; Tables 2 and 4). We found that the synergistic tumorigenic capability of three sub-clones is better than that of any monoclone.

We observed that one mice in $CD19^-/IgM^+$ group (cell inoculation dose: 10^4/mouse) from *JeKo-1-spheroid* had two infected organs and three hemorrhagic organs (Fig. 6D,E; Table 4). One mice in the $CD19^-/IgM^-$ group (cell inoculation dose: 10^4/mouse) from *JeKo-1-spheroid* had one infected organ and one hemorrhagic organ (Table 4). However, no mice in $CD19^+/IgM^+$ group from *JeKo-1-spheroid* was infected and bleeding (cell inoculation dose: 10^2/mice and 10^4/mice, Table 4). In contrast, two mice in $CD19^-/IgM^+$ from pt4 group at 10^2 and 10^4 doses of tumor cell inoculation had two and six infected and hemorrhagic organs, respectively (Fig. 6D,E; Table 4). Two mice in $CD19^+/IgM^+$ from pt4 group at 10^2 and 10^4 doses of tumor cell inoculation had two and three infected and hemorrhagic organs, respectively (Fig. 6D,E; Table 4). However, no infected and hemorrhagic organs were observed in $CD19^-/IgM^-$ group from pt4 group (cell inoculation dose: 10^2/mouse) (Table 4). Two mice in $CD19^-/IgM^-$group (cell inoculation dose: 10^4/mouse) from pt4 group, a total of five

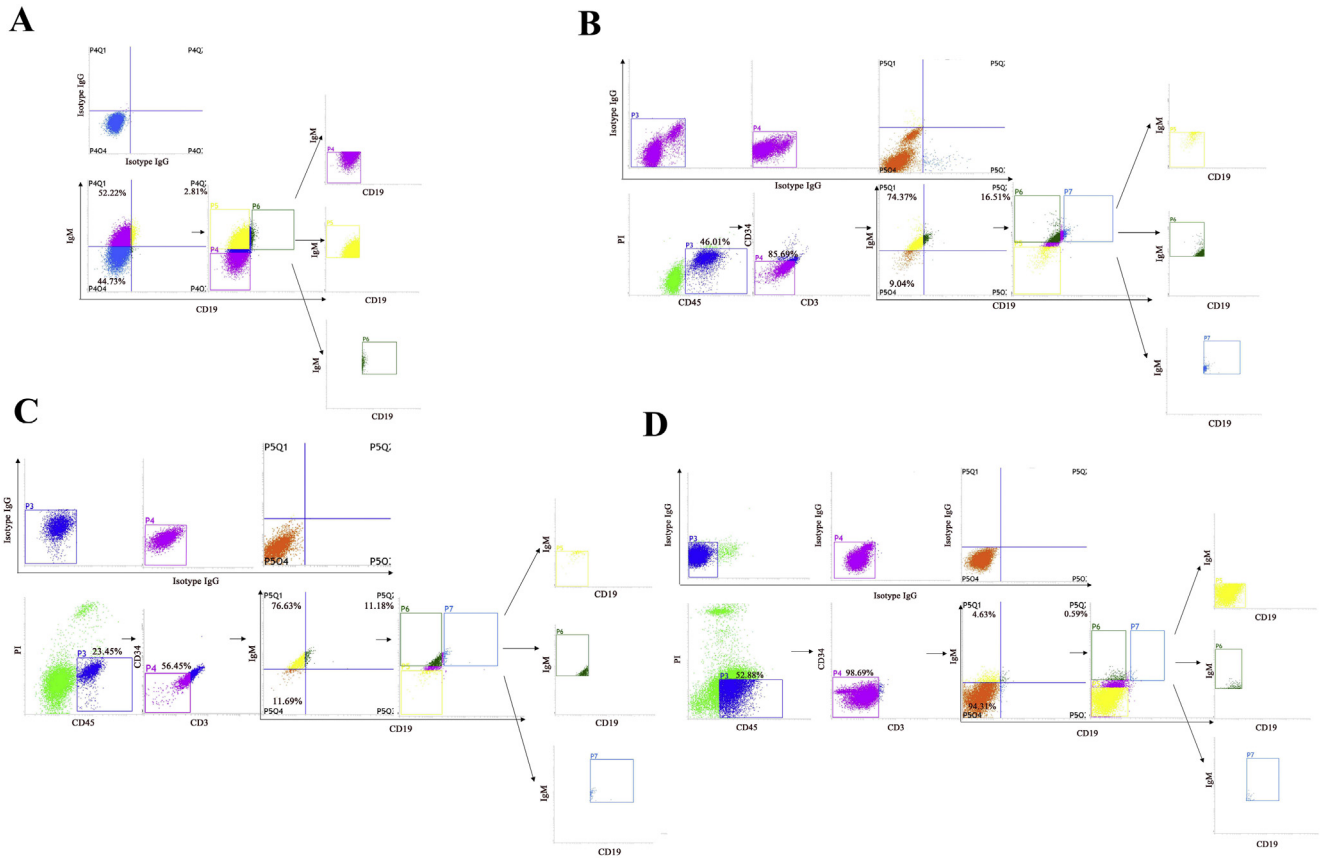

Figure 5 Sorting strategy of three sub-clones derived from patients and *JeKo-1-spheroid* cell line. Isolation of $CD19^-/IgM^-$, $CD19^-/IgM^+$ and $CD19^+/IgM^+$ sub-clones from the *JeKo-1-spheroid* cell line (A), pt1 (B), pt2 (C) and pt4 (D).

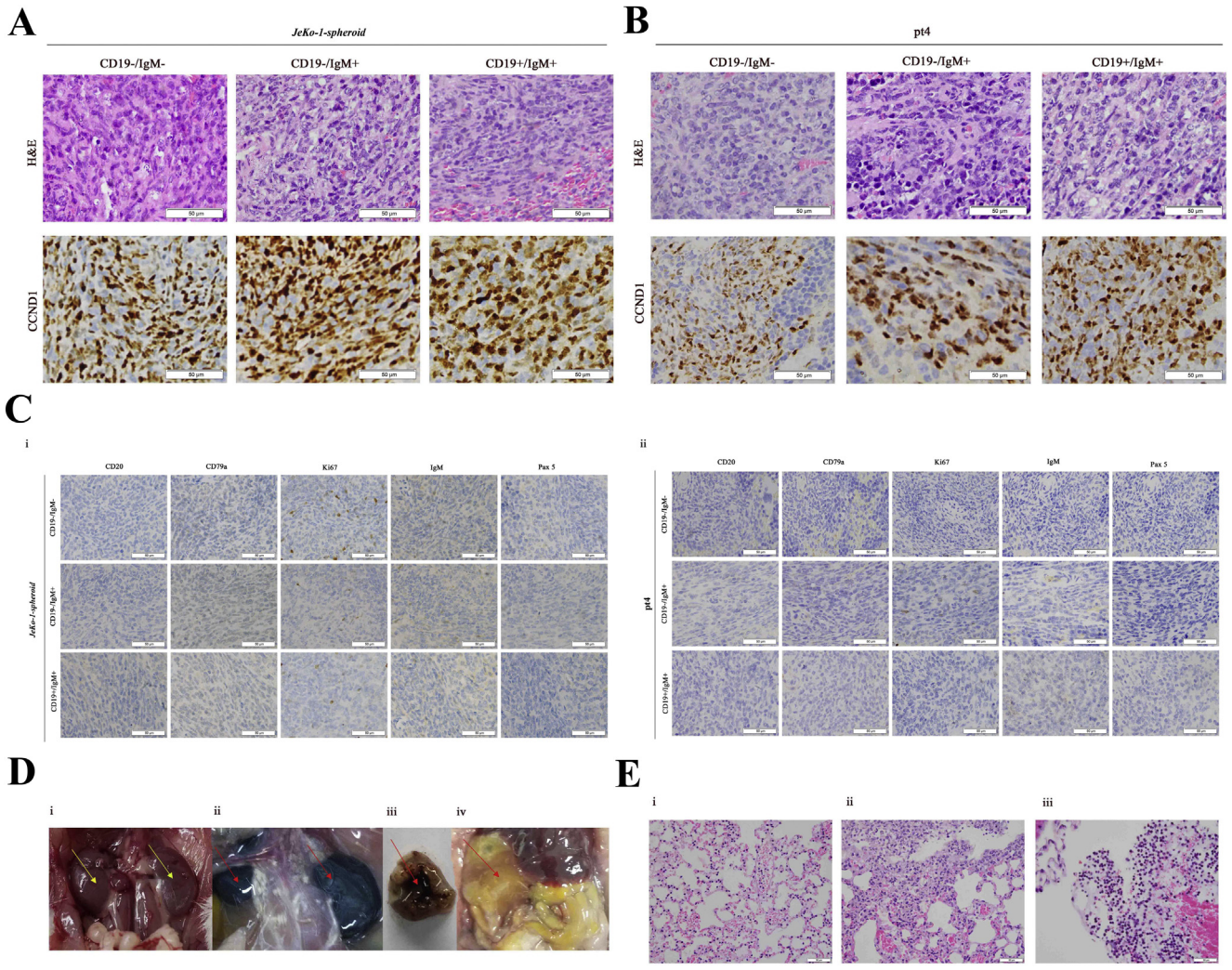

Figure 6 Cancer biology of three sub-clones derived from patients and JeKo-1-spheroid cell line *in vivo*. **(A)** H&E staining and CCND1 immunohistochemistry of the three sub-clones in the *JeKo-1-spheroid*. **(B)** H&E staining and CCND1 immunohistochemistry of the three sub-clones from pt4. **(C)** IHC for the indicated markers in the three sub-clones isolated from *JeKo-1-spheroid* (i) and pt 4 (ii). **(D)** Haemorrhagic and infection manifestations induced by the $CD19^{-}/IgM^{+}$ subclone in NOD/SCID mice. Yellow arrows indicate the normal kidneys (i), red arrows indicate the haemorrhagic kidneys in *JeKo-1-spheroid* (ii), blood can be seen in the stomach from pt4 (iii), and infectious intestine was yellow and formed yellow encapsulated abscesses in pt4 (iv). **(E)** H&E analysis of pulmonary infection and hemorrhage from the three subclones in pt 4: $CD19^{-}/IgM^{-}$ (i); $CD19^{-}/IgM^{+}$ (ii); $CD19^{+}/IgM^{+}$ (iii).

organs were infected and hemorrhagic (Fig. 6E; Table 4). Thus, the $CD19^{-}/IgM^{+}$ sub-clone from either *JeKo-1-spheroid* or pt4 was more likely to develop widespread organ infection and bleeding when compared to the other monoclone (Fig. 3D, E). $CD19^{-}/IgM^{+}$ sub-clone exhibited the strongest tumorigenic ability, more aggressive course of MCL progression (extensive bleeding and infection) and more severe effects on normal hematopoietic and immune functions. Finally, these findings suggest that MCL may be primarily $CD19^{-}/IgM^{+}$-dependent and appears to follow a polyclonal course of pathogenesis.

Discussion

Since worldwide recognition of MCL in 1994, it is known for its dismal prognosis, with a median overall survival (OS) rate of 3 years. The lack of clinically relevant cellular models and effective research methods have hindered in-depth mechanistic investigation of MCL.

It is widely believed that blood cells grow as single cell suspension *in vitro*.[5,12,13,15,16] However, spheroid growth has been a characteristic feature of stem-like cells isolated from solid tumor in serum-free culture condition.[19] In this report, we demonstrate that growth as multicellular spheroid is a unique feature of early-stage cells in MCL. In contrast to multicellular spheroid growth mode of non-blood cancer stem cell that requires the switch of serum culture medium into serum free medium,[19,20] spheroid growth of MCL can be maintained in the same culture condition that contains serum.

The *JeKo-1-parental* cell line, established from PBMCs of a terminal stage MCL patient with a large cell variant of

Table 4 Analysis of tumor xenograft induction in NOD/SCID mice by *JeKo-1- spheroid* and pt4-derived sub-clones.

Cell	Sub-population	Dose	# of mice with tumours	# of infected organs	# of hemorrhagic organs
Jeko-1-spheroid	$CD19^-/IgM^-$	100	3/3	0/33	0/33
		10000	3/3	1/33	1/33
	$CD19^-/IgM^+$	100	3/3	0/33	0/33
		10000	3/3	2/33	3/33
	$CD19^+/IgM^+$	100	3/3	0/33	0/33
		10000	3/3	0/33	0/33
Pt4	$CD19^-/IgM^-$	100	4/4	0/44	0/44
		10000	4/4	5/44	5/44
	$CD19^-/IgM^+$	100	4/4	2/44	2/44
		10000	4/4	6/44	6/44
	$CD19^+/IgM^+$	100	4/4	2/44	2/44
		10000	4/4	3/44	3/44

MCL showing leukemic conversion, similar to pt4 used in our study.[16] Interestingly, when the *JeKo-1-parental* cell line was originally cultured *in vitro*, multicellular spheroid mode of growth was documented. After the first two months, the established cell line adopted the single-cell suspension growth.[16] This observations indicate that when MCL cells were initially isolated from patient, their growth *in vitro* retained the cluster aggregation feature. Single-cell suspension growth maybe a gradual adaptive feature of long-term culture *in vitro*, retaining a very low proportion of early immature cells B cells via multicellular spheroid growth. Differentiation of progenitor B cells is regulated by mature B cells *in vivo*, as decrease in the number of mature B cells in the peripheral blood can stimulate early B progenitor differentiation.[28] This theory consistent with our observation that the death of a large number of single mature B cells stimulated the growth and enrichment of early-stage B cells with spheroid growth (Fig. 1A, C). We speculate that under similar condition, early-stage cells of other hematopoietic tumors could also been enriched by spheroid growth. Future studies will explore whether this experimental approach can be used to establish the clinically relevant cellular models of other hematological cancers for the study of clonal evolution and heterogeneity.

The various features of *JeKo-1-spheroid* such as the spheroid growth mode, enrichment of $CD19^-$ and SP cells, high expression of oncogenes and stem cell markers, enhanced tumorigenic and metastatic capability *in vivo*, high incidence of infection and bleeding better recapitulate the clinical features of MCL. Employment of the *JeKo-1-spheroid* cell line model yielded a set of original findings:

First, MCL might be a polyclonal disease, and $CD19^-/IgM^+$ might be the dominant sub-clone. The three sub-clones ($CD19^-/IgM^-$,$CD19^-/IgM^+$, $CD19^+/IgM^+$) were present in both *JeKo-1-spheroid* cells and MCL clinical samples, among which the $CD19^-/IgM^+$ sub-clone is the dominant clone. Further, the monoclonal tumors retaining only CCND1 expression and mantle zone growth pattern feature of MCL *in vivo*, which consistent with *in situ* mantle cell neoplasia (ISMCN).[10,29] ISMCN is a very indolent tumor and may not require therapeutic intervention. The monoclonal tumors were incapable of manifesting the full pathological phenotypes of clinical MCL when compared to the polyclonal tumors of *JeKo-1-spheroid* cell line. Our results are similar to those of breast cancer studies,[7] that none of the monoclone were metastatic. This finding indicates that CCND1 high expression is necessary at the initiation of MCL, but not sufficient to attain the full scope of pathologic phenotypes.[1,30]

Second, MCL maybe derived from pre-B, immature-B and mature-B cells. Our findings have moved the MCL initiating cell differentiation stage earlier to the pre-B and immature-B stages. MCL was classified as a mature-B cell neoplasm according to the latest WHO classification published in 2016.[10] Current diagnosis of MCL and residual disease after treatment is mainly based on $CD19^+/IgM^+$ and other B cell markers. Expanded clinical cohorts are required to confirm this finding.

Third, $CD19^+/IgM^-$ that differentiates MCL and normal B cells may represent a new clinical marker. We found that the $CD19^+/IgM^-$subgroup was only present in normal B cells (Fig. 4A; Table 3). Expanded clinical cohorts are required to validate the diagnostic and prognostic importance of $CD19^+/IgM^-$.

In summary, our work provides a method for the enrichment of early-stage cells and experimental basis for the polyclonal nature of MCL pathogenesis which may yield improved diagnosis and prognosis, as well as a new path for developing more effective treatment for MCL. We plan to initiate new studies directed at investigating mechanisms regulating clonal evolution and the chemo-resistant of the sub-clones. This will ultimately lead to improved outcomes for MCL patients.

Conflicts of interest

The authors declare no potential conflict of interest.

Acknowledgments

We thank all the patients, healthy donors and their families, as well as The Affiliated Hospital of Southwest Medical

University and Mianyang central hospital participating in this trial. We are thankful to the members in the Laboratory of Translational Cancer Stem Cell Research who are not listed in the authors. This work was funded by the National Natural Science Fund (Grant No. 81272405); the Funds for Luzhou Medical College Applied Basic Research Plan (Grant No. 2015-YJ122); the Key Research Project from Health and Family Planning Commission of Sichuan Province (Grant No. 18ZD014); the National Natural Science Fund (Grant No. 81450030); the Key Research Project of Sichuan Education Department (Grant No. 14ZA0141); the Luzhou Science and Technology Project (Grant No. 2014-S-47).

References

1. Belderbos ME, Koster T, Ausema B, et al. Clonal selection and asymmetric distribution of human leukemia in murine xenografts revealed by cellular barcoding. *Blood*. 2017;129:3210—3220.
2. Shlush LI, Mitchell A, Heisler L, et al. Tracing the origins of relapse in acute myeloid leukaemia to stem cells. *Nature*. 2017;547:104—108.
3. Welch JS, Ley TJ, Link DC, et al. The origin and evolution of mutations in acute myeloid leukemia. *Cell*. 2012 Jul 20;150(2):264—278.
4. Schneider S, Crescenzi B, Schneider M, et al. Subclonal evolution of a classical Hodgkin lymphoma from a germinal center B-cell-derived mantle cell lymphoma. *Int J Cancer*. 2014;134:832—843.
5. Chen Z, Ayala P, Wang M, et al. Prospective isolation of clonogenic mantle cell lymphoma initiating cells. *Stem Cell Res*. 2010;5:212—225.
6. Liu F, Yoshida N, Suguro M, et al. Clonal heterogeneity of mantle cell lymphoma revealed by array comparative genomic hybridization. *Eur J Haematol*. 2013 Jan;90(1):51—58.
7. Marusyk A, Tabassum DP, Altrock PM, Almendro V, Michor F, Polyak K. Non-cell-autonomous driving of tumour growth supports sub-clonal heterogeneity. *Nature*. 2014;514:54—58.
8. Walter HS, Rule SA, Dyer MJ, et al. A phase 1 clinical trial of the selective BTK inhibitor ONO/GS-4059 in relapsed and refractory mature B-cell malignancies. *Blood*. 2016;127:411—419.
9. Zamò A, Ott G, Katzenberger T, et al. Establishment of the MAVER-1 cell line, a model for leukemic and aggressive mantle cell lymphoma. *Haematologica*. 2006 Jan;91(1):40—47.
10. Swerdlow SH, Campo E, Pileri SA, et al. The 2016 revision of the World Health Organization classification of lymphoid neoplasms. *Blood*. 2016 May 19;127(20):2375—2390.
11. Medina DJ, Abass-Shereef J, Walton K, et al. Cobblestone-Area Forming Cells Derived from Patients with Mantle Cell Lymphoma Are Enriched for CD133+ Tumour-Initiating Cells. *PLoS One*. 2014;9, e91042.
12. Matsui W, Huff CA, Wang Q, et al. Characterization of clonogenic multiple myeloma cells. *Blood*. 2004;103:2332—2336.
13. Aoki Y, Watanabe T, Saito Y, et al. Identification of CD34+ and CD34- leukemia-initiating cells in MLL-rearranged human acute lymphoblastic leukemia. *Blood*. 2015;125:967—980.
14. Maurer MJ, Cerhan JR, Katzmann JA, et al. Monoclonal and polyclonal serum free light chains and clinical outcome in chronic lymphocytic leukemia. *Blood*. 2011;118:2821—2826.
15. Ahrens AK, Chaturvedi NK, Nordgren TM, Dave BJ, Joshi SS. Establishment and characterization of therapy-resistant mantle cell lymphoma cell lines derived from different tissue sites. *Leuk Lymphoma*. 2012;53:2269—2278.
16. Jeon HJ, Kim CW, Yoshino T, Akagi T. Establishment and characterization of a mantle cell lymphoma cell line. *Br J Haematol*. 1998;102:1323—1326.
17. Rasmussen T, Jensen L, Honoré L, Johnsen HE. Frequency and kinetics of polyclonal and clonal B cells in the peripheral blood of patients being treated for multiple myeloma. *Blood*. 2000;96:4357—4359.
18. Goodell MA, Brose K, Paradis G, Conner AS, Mulligan RC. Isolation and functional properties of murine hematopoietic stem cells that are replicating in vivo. *J Exp Med*. 1996;183:1797—1806.
19. Qiang L, Yang Y, Ma YJ, et al. Isolation and characterization of cancer stem like cells in human glioblastoma cell lines. *Cancer Lett*. 2009 Jun 28;279(1):13—21.
20. Wang R, Lv Q, Meng W, et al. Comparison of mammosphere formation from breast cancer cell lines and primary breast tumours. *J Thorac Dis*. 2014 Jun;6(6):829—837.
21. Jakubikova J, Adamia S, Kost-Alimova M, et al. Lenalidomide targets clonogenic side population in multiple myeloma: pathophysiologic and clinical implications. *Blood*. 2011 Apr 28;117(17):4409—4419.
22. Braylan RC, Orfao A, Borowitz MJ, Davis BH. Optimal number of reagents required to evaluate hematolymphoid neoplasias: results of an international consensus meeting. *Cytometry*. 2001 Feb 15;46(1):23—27.
23. Khanna R, Belurkar S, Lavanya P, Manohar C, Valiathan M. Blastoid variant of mantle cell lymphoma with leukemic presentation — A rare case report. *J Clin Diagn Res*. 2017 Apr;11(4):ED16—ED18.
24. Zapata M, Budnick SD, Bordoni R, Li S. An uncommon case of de novo CD10+ CD5- mantle cell lymphoma mimics follicle center B cell lymphoma. *Int J Clin Exp Pathol*. 2010 Mar 20;3(4):430—436.
25. Pérez-Galán P, Dreyling M, Wiestner A. Mantle cell lymphoma: biology, pathogenesis, and the molecular basis of treatment in the genomic era. *Blood*. 2011 Jan 6;117(1):26—38.
26. Chisholm KM, Bangs CD, Bacchi CE, Molina-Kirsch H, Cherry A, Natkunam Y. Expression profiles of MYC protein and MYC gene rearrangement in lymphomas. *Am J Surg Pathol*. 2015 Mar;39(3):294—303.
27. Campo E, Raffeld M, Jaffe ES. Mantle cell lymphoma. *Semin Hematol*. 1999;36:115—127.
28. Shahaf G, Zisman-Rozen S, Benhamou D, Melamed D, Mehr R. B cell development in the bone marrow is regulated by homeostatic feedback exerted by mature B cells. *Front Immunol*. 2016;7:77.
29. Carvajal-Cuenca A, Sua LF, Silva NM, et al. In situ mantle cell lymphoma: clinical implications of an incidental finding with indolent clinical behavior. *Haematologica*. 2012 Feb;97(2):270—278.
30. Jares P, Colomer D, Campo E. Molecular pathogenesis of mantle cell lymphoma. *J Clin Invest*. 2012 Oct;122(10):3416—3423.